

# Apparent nonergodic behavior of supercooled liquids above the glass transition temperature

A. Patkowski,<sup>1,2</sup> H. Gläser,<sup>1</sup> T. Kanaya,<sup>3</sup> and E. W. Fischer<sup>1</sup>

<sup>1</sup>Max Planck Institute for Polymer Research, Ackermannweg 10, 55128 Mainz, Germany

<sup>2</sup>Institute of Physics, A. Mickiewicz University, Umultowska 85, 61-614 Poznan, Poland

<sup>3</sup>Institute for Chemical Research, Kyoto University, Uji, Kyoto-fu 611, Japan

(Received 2 January 2001; published 29 August 2001)

A speckle pattern can be observed in the polarized component of light scattered from glass forming liquids far above their glass transition temperature. This speckle pattern fluctuates with characteristic time that corresponds to the relaxation time of the additional ultraslow component in the correlation function and is about seven orders of magnitude longer than the relaxation time of the  $\alpha$ -process. This slow process is out of the experimental time window when the  $\alpha$ -process is measured by means of the photon correlation spectroscopy and results in an apparent nonergodicity which can be seen as a baseline offset in the ensemble-averaged correlation function. In contrast, the time-averaged field correlation functions which have been measured in practically all light scattering studies always decay to zero. The slow process contributes a  $q$ -dependent excess intensity to the polarized component of scattered light. The values of the nonergodicity parameters obtained from the static and dynamic light scattering experiments are equal. Both the slow component and the excess intensity result from denser regions of fractal character which develop in glass-forming liquids on approaching the glass transition.

DOI: 10.1103/PhysRevE.64.031503

PACS number(s): 64.70.Pf, 78.35.+c

## I. INTRODUCTION

One of the important questions in the field of supercooled liquids concerns their structural and dynamic heterogeneity. Before trying to answer this question, first we have to define the time and length scale under consideration. Experimental evidence for a dynamically heterogeneous character of low molecular weight and polymeric glass forming liquids on the length scale of the order of 1 nm has been accumulated using selective photobleaching [1], multidimensional nuclear magnetic resonance (NMR) and dielectric spectroscopy (hole burning), and extensively reviewed [2,3]. Recently, it has been shown in molecular dynamics simulations for Lennard-Jones liquids that spatial correlations between the displacements of molecules become increasingly long on approaching the mode-coupling temperature  $T_c$  [4]. Other simulations of monoatomic liquids revealed that the number of icosahedral clusters increases with decreasing temperature [5]. The dynamics of low molecular weight and polymeric glass forming liquids has been extensively studied by dynamic light scattering (DLS, PCS) [6,7]. In all those studies only the time-averaged correlation functions in the time range appropriate for the primary ( $\alpha$ )-relaxation have been measured. Previously it has been shown [8] that the time correlation function corresponding to density fluctuations does not decay to zero due to an additional slow process of a relaxation time  $\tau_{\text{slow}} \cong 10^7 \tau_\alpha$ . This slow process contributes only to the isotropic component of scattered light since it is not observed in the dynamic depolarized (VH) light scattering. It is believed that the ultra slow modes are due to the dynamics of the long-range density fluctuations which have been established as a universal feature of polymeric and low molecular glass forming liquids above  $T_g$  [8–10]. They appear in static light scattering (SLS) as an additional  $q$ -dependent isotropic intensity contribution in addition to the  $q$ -independent intensity related to the isothermal compress-

ibility. The amount of the excess scattering can exceed the amount due to isothermal compressibility by a factor of 100 depending on temperature and scattering angle. An evaluation of the SLS data according to an Ornstein-Zernike correlation function yields correlation lengths in the range of 10 to several hundreds of nanometers. The samples can transiently be prepared in a state without long-range density fluctuations, but the original state will always show up again after some annealing time [8,11]. The additional slow process and the excess scattering in SLS always appear simultaneously, strongly suggesting that they have the same origin. The long-range density fluctuations were originally discovered in static light scattering measurements in the  $q$ -range  $7 \times 10^{-3}$  to  $4 \times 10^{-2} \text{ nm}^{-1}$ . Recently [12], it was shown that they also can be detected by ultra small angle x-ray scattering (USAXS) using synchrotron radiation at the ESRF, Grenoble. The relaxation time of the slow process is usually out of the window of the correlator at temperatures where the  $\alpha$ -process is measured and has not been seen in most of the previous work. The slow process can lead to apparent nonergodic time averaged correlation functions on the time scale of the  $\alpha$ -process, because the  $\alpha$ - and the slow processes are separated in time by several orders of magnitude. At sufficiently low temperatures the slow process is out of the window of the correlator within reasonable measurement times. Under such conditions the baseline of the time-averaged correlation function is seemingly not shifted, but the contrast of the correlation function will be reduced. Contrary to that an ensemble-averaged correlation function will show a baseline shift. Hence, the ensemble-averaged and time-averaged correlation functions of the  $\alpha$ -process are not equal, as it has been measured for samples with long-range density fluctuations by us. That is what we call “apparent nonergodicity on the time scale of the  $\alpha$ -process.” This nonergodicity has nothing to do with the nonergodicity predicted by the mode-coupling theory (MCT) [13] which should occur at  $T_c$  on a

much faster time scale between the  $\beta$ -regime and the  $\alpha$ -(hopping) process. Thus our nonergodicity occurs on a time scale about 10 orders of magnitude slower than the nonergodicity predicted by the MCT. In this paper a systematic comparison of the time- and ensemble-averaged correlation functions for low molecular weight glass forming liquids is presented. We show that the apparent nonergodicity is due to the long-range density fluctuations. The influence of the apparent nonergodicity on the measurement of the relaxation times of the  $\alpha$ -process and of the static intensity is discussed.

## II. THEORETICAL BACKGROUND

In dynamic light scattering experiments two normalized time autocorrelation functions are considered: the first order (field) autocorrelation function

$$g^{(1)}(\tau) = \frac{\langle E^*(0)E(\tau) \rangle}{\langle E^2 \rangle}, \quad (1)$$

and the second order (intensity) autocorrelation function

$$g^{(2)}(\tau) = \frac{\langle I(0)I(\tau) \rangle}{\langle I \rangle^2}. \quad (2)$$

Both correlation functions can represent either time-averaged  $\langle \rangle_t$  or ensemble-averaged  $\langle \rangle_E$  quantities. The instantaneous state of the system of  $f$  degrees of freedom is defined by  $f$  generalized positions  $(q_1, \dots, q_f)$  and momenta  $(p_1, \dots, p_f)$ :  $\Gamma_t \equiv (q_1(t), \dots, p_f(t))$ . The not normalized ensemble-averaged time autocorrelation function of a property  $A(t)$  is defined as

$$G_E(\vec{q}, t) \equiv \langle A(0)A(t) \rangle_E \equiv \int d\Gamma_0 \rho(\Gamma_0) A(\Gamma_0) A(\Gamma_t), \quad (3)$$

where  $A(\Gamma_0)$  and  $A(\Gamma_t)$  are properties of the system defined as functions of the instantaneous states  $\Gamma_0$  and  $\Gamma_t$ , respectively,  $\rho(\Gamma_0)$  is the probability of finding the system in the initial state  $\Gamma_0$ . A time average of any function  $F\{A(t)\}$  of a variable  $A(t)$  randomly varying in time is defined as

$$\langle F\{A(t)\} \rangle_t = \lim_{T \rightarrow \infty} \frac{1}{T} \int_0^T dt F\{A(t)\}. \quad (4)$$

In practice  $\infty$  in the  $\lim_{T \rightarrow \infty}$  is replaced by  $T_\infty$ , which is the experimental (averaging) time and in light scattering experiments it is of the order of minutes or hours. It is sufficient if  $T_\infty \gg \tau_l$  ( $\tau_l$  being the longest relaxation time in the system). For an ergodic system  $\langle \rangle_t = \langle \rangle_E$ , where the indices  $t$  and  $E$  denote the time- and ensemble-average, respectively. If we have two processes in the system:  $\tau_1 \ll T_\infty$  and  $\tau_2 = \tau_l > T_\infty$  then the system is apparently nonergodic on the time scale of  $\tau_1$ . Obviously, this nonergodicity can be seen only if the time- and ensemble-averaged correlation functions are measured at the same time under the same conditions. The features of a nonergodic system observed in a light scattering experiment have been extensively discussed [14,15] and can

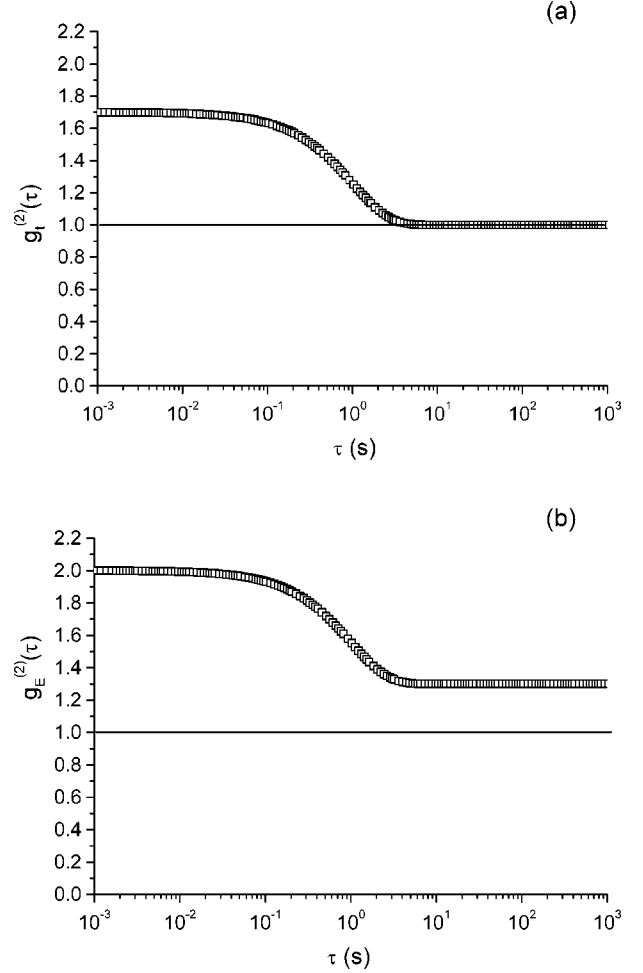


FIG. 1. (a) Time-averaged and (b) ensemble-averaged normalized intensity correlation function for a nonergodic system.

be summarized as follows: (i) Strong fluctuations of the scattered intensity in space (different positions in the sample). (ii) Fluctuating contrast of the time-averaged correlation function  $g_t(\vec{q}, t)$  depending on position in the sample. (iii)  $g_t^{(1,2)}(\vec{q}, t) \neq g_E^{(1,2)}(\vec{q}, t)$  and the ensemble-averaged correlation functions exhibit baseline shift:  $g_E^{(2)}(\vec{q}, \infty) > 1$  and  $g_E^{(1)}(\vec{q}, \infty) > 0$ . The intensity correlation function for a nonergodic system is shown in Fig. 1 [14]: If there are no faster processes out of the window of the correlator the time averaged correlation function  $g_E^{(2)}(\tau)$  starts from a value less than 2 for  $\tau=0$  and decays to a usual baseline of 1 at  $\tau=\infty$ . The ensemble-averaged correlation function starts from 2 at  $\tau=0$  but exhibits a baseline offset  $g_E^{(2)}(\infty) > 1$  at  $\tau=\infty$ . For an ergodic system both time- and ensemble averaged correlation functions are equal and decay from 2 at  $\tau=0$  to 1 at  $\tau=\infty$ .

## III. EXPERIMENT

### A. Light scattering measurements

The static light scattering (SLS) and photon correlation spectroscopy (PCS) measurements were performed using an experimental setup described elsewhere [9]. A vertically po-

larized beam from a krypton ion laser (Spectra Physics, model 2020),  $\lambda = 647$  nm, was focused in the scattering volume. The scattered light, after passing an analyzer and two pinholes (0.4 mm diameter) was detected by a photomultiplier (EMI 9863KA/100) working in the photon-counting mode. The measurements were performed using the ALV goniometer (ALV-Laservertriebsgesellschaft, Langen, Germany), modified in our laboratory to be able to cover an extended temperature range from  $-40$  to  $130^\circ$  C, and ALV-5000 fast correlator. A Glan prism (Halle, Berlin) with an extinction coefficient better than  $10^{-6}$  was used as a polarizer in the incident beam and a Glan-Thompson prism (Halle, Berlin) of the extinction coefficient better than  $10^{-7}$  was used as an analyzer in the scattered beam. In order to measure the ensemble-averaged intensity and correlation functions by rotating the sample [15] a rotating cell holder has been designed. The ensemble-averaged intensity was obtained by rotating the sample (at a speed of 10 rpm) during the SLS measurement, i.e., at each scattering angle 3 or 5 measurements of 3 or 5 seconds duration were taken and the average value was calculated. Such a measurement resulted always in a much smoother SLS data than the one obtained with a stationary sample [8]. In order to obtain the ensemble-averaged correlation function up to 250 time-averaged correlation functions have been measured. After each measurement the sample was rotated by an angle, which was computed by a random number generator. The ensemble-averaged correlation function was obtained as a sum of these 250 not-normalized correlation functions. Such procedure was previously found to produce a very close estimate of the ensemble-averaged correlation function [15].

### B. Sample preparation

Ortho-terphenyl (OTP) was bought from Merck-Schuchardt, several times recrystallized from methanol solution and distilled under vacuum into dust-free light scattering cells (round 10–20 mm outer diameter). The purified OTP showed a melting temperature  $T_m$  of 328.5 K and a glass transition temperature [measured by means of differential scanning calorimetry (DSC) at a cooling rate of 10 K/min] amounted to  $T_g = 244.8$  K in a good agreement with the literature data [16]. The BMMPC [1,1-di(4-methoxy-5methyl-phenyl)-cyclohexane] samples were synthesized in our laboratory following the procedure given in Ref. [17]. The melting temperature of BMMPC amounted to  $T_m = 346$  K and the glass transition temperature, measured by means of DSC at a cooling rate of 10 K/min amounted to  $T_g = 261$  K. The samples were filtered three times at 353 K through a  $0.22 \mu\text{m}$  Millipore filter into dust free cylindrical cells made out of Pyrex tubes. Distillation of BMMPC into the light scattering cell was not possible due to decomposition of the sample beyond 370 K which is below the boiling point under high vacuum. Poly(methyl-*p*-tolylsiloxane) (PMpTS) of molecular weight  $M_w = 1.5 \times 10^4$  was synthesized and purified in our laboratory as described elsewhere [18]. The molecular weight distribution  $M_w/M_n$  measured by GPC amounted to 1.09. The glass transition temperature measured by DSC amounted to 256 K. The light scattering

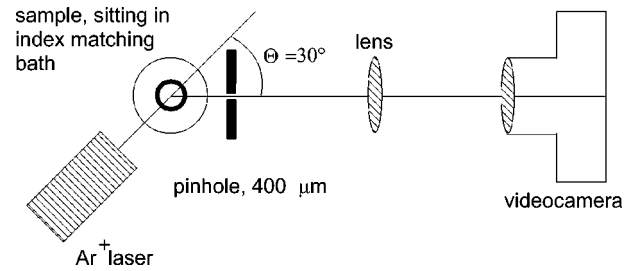


FIG. 2. Optical setup used to record the fluctuations of the speckle pattern.

sample was prepared by filtering PMpTS through a  $0.22 \mu\text{m}$  Millipore filter directly into the light scattering cell at 393 K.

## IV. RESULTS AND DISCUSSION

### A. Static light scattering

One of the commonly observed and (until recently) ignored features of low molecular weight and polymeric glass forming liquids are strong fluctuations of the polarized (VV) scattered intensity in a temperature range from the glass transition temperature  $T_g$  to the melting temperature  $T_m$  and in some cases even for  $T > T_m$ . In order to investigate these fluctuations in some more detail but still on a qualitative level we have recorded the speckle pattern with a CCD camera using the optical setup shown schematically in Fig. 2 [19]. In Fig. 3(a) the speckle pattern observed for OTP at 293 K is shown. This speckle pattern fluctuates very slowly at this temperature with a characteristic time of the order of minutes, that means much longer than the  $\alpha$ -relaxation time ( $\tau_\alpha = 40$  ns). Since in the SLS experiment the pinhole size is comparable to the speckle size the PM tube is registering high fluctuations of the measured intensity of scattered light due to the movements of the speckles through the pinholes. With increasing temperature the speckle size and contrast is decreasing and speckle dynamics is getting faster. This finally leads to a uniform distribution of the scattered intensity (no speckles) at higher temperatures, when the characteristic time of fluctuations of the speckle pattern is shorter than the exposure time of the CCD camera. No speckles (nor fluctuations) can be observed in this temperature range for the depolarized (VH) component of the scattered light. Due to the presence of speckles the time-averaged intensity of scattered light in the SLS experiment exhibits very strong random fluctuations [8] making any quantitative analysis of the experimental data very difficult. A measurement of the ensemble-averaged intensity using a rotating cell reduces dramatically the fluctuations of the signal [8] and only this data should be used for further analysis. All these features suggest that, e.g., a BMMPC sample is nonergodic on the  $\tau_\alpha$  time scale of the experiment in the temperature range from  $T_g$  to  $T_g + 40$  K. Identical behavior has been observed in our laboratory in other glass forming liquids: BMPC [1,1-di(4'-methoxy-phenyl)-cyclohexane], PDE (phenolphthalein-dimethyl-ether), glycerin, PMpTS, PEMS (polyethyl-methyl-siloxane) and in general in all glass-forming liquids in which an excess isotropic intensity due to long-range density fluctuations can be seen. Similar comparative analysis

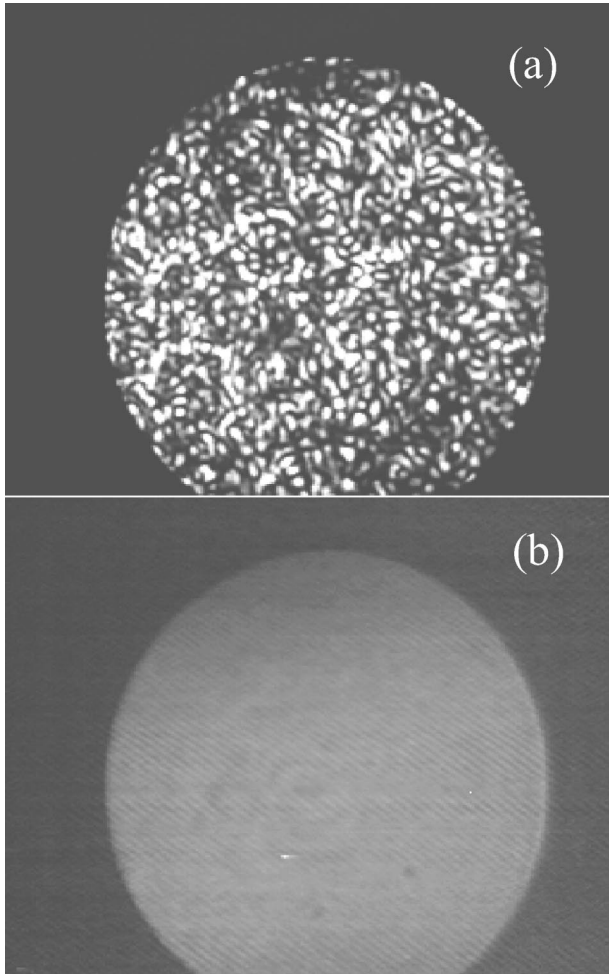


FIG. 3. The speckle pattern obtained at 293 K for OTP with (a) and without (b) long-range density fluctuations (excess scattering).

has been performed for the OTP samples with and without long-range density fluctuations; the latter can be prepared by a special treatment as described in [11]. As one can see in Fig. 3(a) OTP with long-range density fluctuations exhibits a well developed speckle pattern, while at the same temperature of 293 K for the sample without long-range density fluctuations no speckles can be seen [Fig. 3(b)]. This indicates that the apparent nonergodicity of the glass-forming liquids is directly related to long-range density fluctuations which result in an excess isotropic intensity. The fluctuations of the scattered intensity for OTP at 253 K and  $q = 0.023 \text{ nm}^{-1}$  are shown in Fig. 4. Only the polarized (VV) component for OTP with excess scattering exhibits strong fluctuations in time while the depolarized component (VH) for this sample as well as both polarized and depolarized components of the OTP sample without excess scattering show no strong fluctuations.

### B. Time correlation functions

In Fig. 5 the construction of the ensemble-averaged polarized (VV) correlation function for OTP with long-range density fluctuations at 263 K and  $q = 0.014 \text{ nm}^{-1}$  is shown. The time-averaged correlation function (the lowest one, denoted

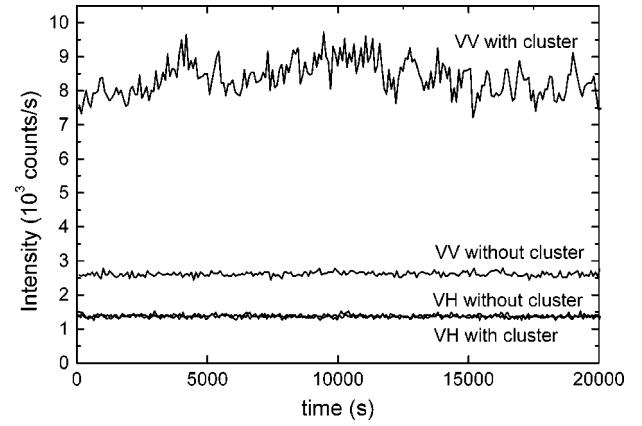


FIG. 4. Time dependence (fluctuations) of the scattered intensity obtained for OTP at 253 K,  $q = 0.023 \text{ nm}^{-1}$ : VV and VH components measured for OTP with and without excess scattering.

1) was accumulated for 30 min. The ensemble-averaged correlation functions represent an average of 5, 10, 50, 100, 150, and 240 time-averaged correlation functions accumulated for 200 s each. Before each subsequent measurement the sample was rotated by a random angle. As it can be seen the averaging of 150 and 240 correlation functions results in a practically identical function which is assumed to be the true ensemble-averaged correlation function [14,15]. From the data shown in Fig. 5 it is clear that this OTP correlation function at 263 K is nonergodic on the time scale of the experiment, i.e.,  $g_t^{(2)}(\vec{q}, t) \neq g_E^{(2)}(\vec{q}, t)$ . The decaying part of the  $g_E^{(2)}(\vec{q}, t)$  is due to the  $\alpha$ -process ( $\tau = 0.60 \text{ ms}$ ) and the baseline offset  $g_E^{(2)}(\vec{q}, \infty)$  is related to the amplitude of the correlation function of a much slower process (i.e., long-range density fluctuations,  $\tau_{\text{slow}} \cong 10^7 \tau_\alpha$ ). This much slower process can be moved into the time window of the correlator by an increase of the temperature and has been studied in detail previously [11]. In most of the previous studies only the time-averaged correlation functions have been measured for glass forming liquids. From such a measurement it is difficult to draw conclusions concerning the ergodicity of the

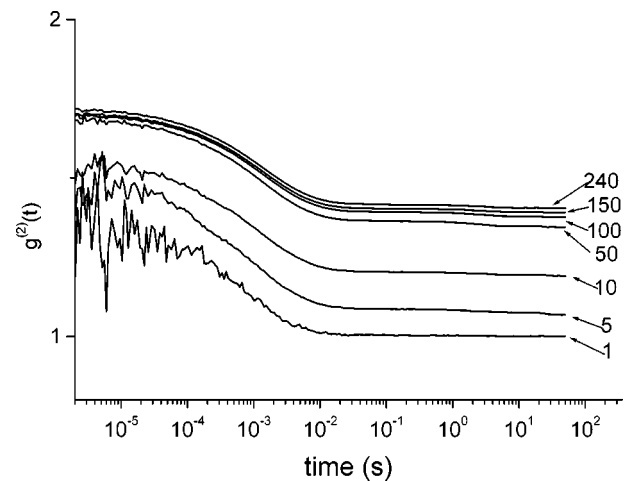


FIG. 5. Construction of the ensemble-averaged correlation function for OTP at 263 K and  $q = 0.014 \text{ nm}^{-1}$ .

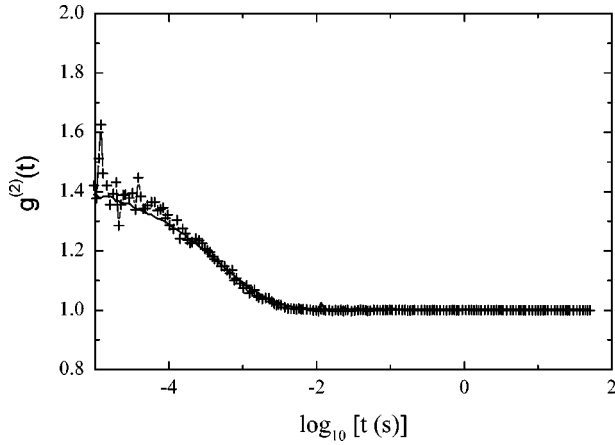


FIG. 6. Time- (+) and ensemble-averaged (solid line) correlation function measured for OTP without excess scattering:  $T = 263$  K,  $q = 0.013$  nm $^{-1}$ .

sample because the time-averaged intensity correlation function always decays to one [14]. The only indications concerning the nonergodicity are fluctuating intensity and reduced contrast of the VV component. These two features may be also caused by other reasons. However, the only way to see the nonergodicity of the sample is to measure the ensemble-averaged correlation function, as it has been done in this study. The time- and ensemble-averaged correlation functions (averaged over 240 runs) measured for OTP without excess scattering at the same temperature (263 K) and scattering angle ( $\Theta = 50^\circ$ ) as in Fig. 5 are shown in Fig. 6. As one can see this OTP sample is ergodic, i.e.,  $g_t(\vec{q}, t) = g_E(\vec{q}, t)$ . Similar picture is obtained when the correlation functions of the depolarized (VH) component of both OTP samples with and without excess intensity are measured. Thus we can conclude that the nonergodic behavior can be seen only in the polarized (VV) component of scattered light for samples with excess scattering and is due to long-range density fluctuations.

### C. Influence of the excess scattering on the relaxation times of the $\alpha$ -process

As discussed in Ref. [14], p.721, evaluating a nonergodic correlation function in an ergodic manner can lead to misinterpretations. This effect can be described as heterodyning of the fluctuating and constant part of the intensity. According to [20] for a heterodyne signal the following expression for the time-averaged intensity correlation function  $g_t^{(2)}(\vec{q}, t)$  holds:

$$g_t^{(2)}(\vec{q}, t) = 1 + \frac{2I_{\text{fluct}}^t I_{\text{exc}}(\vec{q})}{[I_{\text{fluct}}^t + I_{\text{exc}}(\vec{q})]^2} g_t^{(1)}(\vec{q}, t) + \left( \frac{I_{\text{fluct}}^t}{I_{\text{fluct}}^t + I_{\text{exc}}(\vec{q})} \right)^2 |g_t^{(1)}(\vec{q}, t)|^2, \quad (5)$$

with  $I_{\text{fluct}}^t$  being the time-averaged fluctuating intensity and  $I_{\text{exc}}$  is the not-averaged excess scattering resulting from a

distinct speckle of the speckle pattern (Fig. 3). In case of  $I_{\text{exc}} = 0$  one obtains the Siegert relation for homodyne detection, i.e., the term linear in  $g_t^{(1)}(\vec{q}, t)$  does not contribute to  $g_t^{(2)}(\vec{q}, t)$ . In case of  $I_{\text{exc}} \gg I_{\text{fluct}}^t$  only the linear term in  $g_t^{(2)}(\vec{q}, t)$  contributes to the measured intensity correlation function. This may lead to an apparent relaxation time  $\tau_\alpha$  which is by a factor  $2^{1/\beta_{\text{KWW}}}$  higher than the true correlation time. In many cases this may not be important because of the dramatic change of  $\tau_\alpha$  with temperature. It has to be taken into account, however, if the DLS relaxation times are compared with those from other measurements, i.e., dielectric relaxation at the same temperature.

### D. Relation between slow mode and excess intensity

In the case of apparent nonergodicity the ensemble-averaged field correlation function  $g_E^{(1)}(\vec{q}, t)$  does not decay to zero in the time window of the experiment. Therefore, one can define a dynamic nonergodicity parameter:

$$f_{\text{dyn}}(q) = \lim_{t \rightarrow \infty} g_E^{(1)}(\vec{q}, t) \quad (6)$$

which can be compared with the static light scattering data [15]. For that purpose we divide the ensemble-averaged polarized (VV) intensity into a nonfluctuating part  $I_{\text{exc}}^E(\vec{q})$  and a fluctuating part  $I_{\text{fluct}}^E(\vec{q}, t)$ :

$$I_{\text{VV}}^E(\vec{q}, t) = I_{\text{exc}}^E(\vec{q}) + I_{\text{fluct}}^E(\vec{q}, t). \quad (7)$$

$I_{\text{fluct}}^E(\vec{q}, t)$  is related to the isothermal compressibility (or to the short-range density fluctuations) and to the reorientation of the molecules. Experiments show that  $I_{\text{fluct}}^E(\vec{q}, t)$  does not depend on the scattering vector  $q$  in the light scattering window and even not in the conventional SAXS range [12]. The static nonergodicity parameter can be defined by

$$f_{\text{stat}}(q) = \frac{I_{\text{exc}}^E(\vec{q})}{I_{\text{exc}}^E(\vec{q}) + I_{\text{fluct}}^E(\vec{q}, t)}. \quad (8)$$

In Fig. 7 values of  $f_{\text{stat}}(q)$  obtained from BMMPC at 295 K in dependence on  $q^2$  using Eq. (8) are compared with values of  $f_{\text{dyn}}(q)$  directly obtained from ensemble-averaged VV intensity correlation functions. The latter values were obtained by fitting the ensemble-averaged intensity correlation functions  $g_E^{(2)}(\vec{q}, \infty)$  to the Siegert relation:

$$g_E^{(2)}(\vec{q}, t) = 1 + |g_E^{(1)}(\vec{q}, t)|^2. \quad (9)$$

The ensemble-averaged correlation functions and the static intensities were measured under the same conditions for the same sample. The agreement between the two ways of obtaining the nonergodicity parameter is quite good. Hence the slow mode is due to the excess scattering.

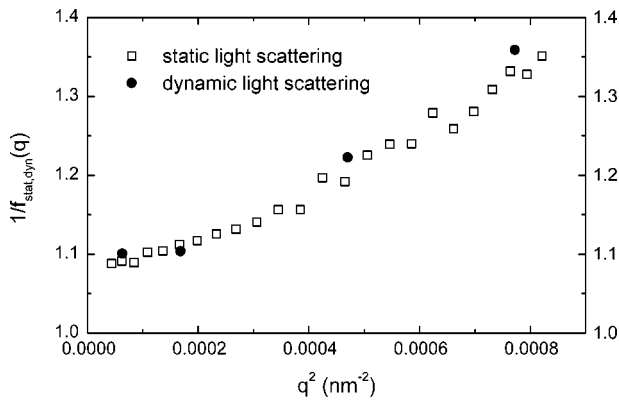


FIG. 7. Comparison of the values of nonergodicity parameter obtained from the static (SLS)  $f_{\text{stat}}(q)$ ,  $\square$ ; and dynamic (PCS)  $f_{\text{dyn}}(q)$ ,  $\bullet$  light scattering experiments.

### E. Physical nature of clusters

In our previous paper [12], we showed that the excess scattered intensity exhibits a power-law  $q$ -dependence in a  $\log_{10}$ - $\log_{10}$  plot of intensity versus  $q$ . In this case (OTP) the power law extended over a substantial  $q$ -range and could be easily identified, because the experimental data covered an unusually broad  $q$ -range of almost two decades due to a combination of the SLS and ultra small angle x-ray scattering (USAXS) data. In order to explain the long-range density fluctuations and the ultraslow dynamical mode a phenomenological model is proposed, which starts from the coexistence of “liquidlike” and “solidlike” regions within the liquid. Such ideas have been discussed many times before [21–25]. Local structures with an energetically preferred configuration (“aperiodic solids” or “glassy clusters”) coexist on a time scale  $t < \tau_\alpha$  with the fluid, where  $\tau_\alpha$  is determined by the escape rate from the local energy minimum in an energy landscape. Molecular dynamics simulations [5,26] of atomic liquids showed that such heterophase fluctuation may appear in the supercooled state. The thermodynamics of such systems has been developed [27–29] and recent x-ray scattering studies [30] clearly demonstrate the coexistence of several structural units in supercooled salol and propylene carbonate. For the explanation of the long-range density fluctuations

we propose that the molecules in the different dynamic states (“liquid” or “solid”) aggregate during annealing of the liquids probably in some fractal manner, where the fractal dimensions can be determined by scattering experiments, at least in principle [12]. The ultraslow mode and the apparent nonergodic behavior described above are caused by the diffusion of the dynamic state, which is coupled to the density. The density autocorrelation function decays very slowly because of the large correlation length.

### V. CONCLUSIONS

The slow process in polymeric and low molecular weight glass forming liquids as seen in a dynamic light scattering experiment near  $T_g$  results in an apparent nonergodicity (on the time scale of the  $\alpha$ -process) observed in the correlation function of the polarized scattered intensity. This is due to the extremely different correlation times of the slow and the  $\alpha$ -process. At lower temperatures the fluctuations of the slow process are frozen in comparison with the time scale of the  $\alpha$ -process. The interference pattern due to the long-range density fluctuations becomes static and can be seen even by eye. This speckle pattern gives rise to an angular dependent excess scattering and seriously disturbs static measurements. The distortion can be removed by rotating the sample. By measuring non-normalized time-averaged correlation functions for different speckles and adding them one obtains a true ensemble average. For OTP at 263 K the averaging of about 240 correlation functions is sufficient. Correlation functions of samples without long-range density fluctuations and correlation functions measured in VH geometry show no nonergodicity. The constant intensity part of the total intensity leads to a heterodyning effect. Due to this heterodyning the correlation times of the time-averaged correlation function are longer than the correlation times of the ensemble-averaged correlation functions. The nonergodicity parameter obtained from ensemble-averaged correlation functions agree quite well with the one obtained by SLS. The long-range spatial heterogeneities observed in glass forming liquids (clusters) can be modeled as fractal aggregates of more dense regions.

- 
- [1] C. Y. Wang and M. D. Ediger, *J. Phys. Chem. B* **103**, 4177 (1999).
- [2] H. Sillescu, *J. Non-Cryst. Solids* **243**, 81 (1999).
- [3] M. D. Ediger, C. A. Angell, and S. R. Nagel, *J. Phys. Chem.* **100**, 1300 (1996).
- [4] C. Bennemann, C. Donati, J. Baschnagel, and S. C. Glotzer, *Nature (London)* **399**, 246 (1999).
- [5] T. Tomida and T. Egami, *Phys. Rev. B* **52**, 3290 (1995).
- [6] *Colloid Polym. Sci.* **91** (1993) (entire volume).
- [7] G. Fytas and G. Meier, in *Dynamic Light Scattering. The Method and Some Applications*, edited by W. Brown (Oxford University Press, Oxford, 1993), pp. 407–439.
- [8] A. Patkowski, E. W. Fischer, H. Gläser, G. Meier, H. Nilgens, and W. Steffen, *Prog. Colloid Polym. Sci.* **91**, 35 (1993).
- [9] E. W. Fischer, G. Meier, T. Rabenau, A. Patkowski, W. Steffen, and W. Thönnies, *J. Non-Cryst. Solids* **131-133**, 134 (1991).
- [10] E. W. Fischer, *Physica A* **201**, 183 (1993).
- [11] A. Patkowski, E. W. Fischer, W. Steffen, H. Gläser, M. Baumann, T. Ruths, and G. Meier, *Phys. Rev. E* **63**, 061503 (2001).
- [12] A. Patkowski, Th. Thurn-Albrecht, E. Banachowicz, W. Steffen, P. Bösecke, T. Narayanan, and E. W. Fischer, *Phys. Rev. E* **61**, 6909 (2000).
- [13] W. Götze and L. Sjögren, *Rep. Prog. Phys.* **55**, 241 (1992).
- [14] P. N. Pusey and W. van Meegen, *Physica A* **157**, 705 (1989).
- [15] J. G. H. Joosten, E. T. F. Gelade, and P. N. Pusey, *Phys. Rev. A* **42**, 2161 (1990).
- [16] R. J. Grest and D. Turnbull, *J. Chem. Phys.* **46**, 1243 (1967).

- [17] B. Gerharz, G. Meier, and E. W. Fischer, *J. Chem. Phys.* **92**, 7110 (1990).
- [18] B. Momper, Ph.D. thesis, Mainz, 1989.
- [19] P. J. Carroll, G. D. Patterson, and S. A. Cullerton, *J. Polym. Sci., Polym. Phys. Ed.* **21**, 1889 (1983).
- [20] *Photon Correlation and Light Beating Spectroscopy*, edited by H. Z. Cummins and E. R. Pike (Plenum, New York, 1976).
- [21] A. R. Ubbelohde, *The Modern State of Matter* (Wiley, New York, 1978).
- [22] C. A. Angell and J. J. Rao, *J. Chem. Phys.* **57**, 470 (1972).
- [23] M. H. Cohen and G. S. Grest, *Phys. Rev. B* **20**, 1077 (1979).
- [24] J. Y. Cavaille, J. Perez, and G. P. Johari, *Phys. Rev. B* **39**, 2411 (1989).
- [25] J. T. Bendler and M. F. Shlesinger, *J. Phys. Chem.* **96**, 3970 (1992).
- [26] D. C. Wallace and B. E. Clements, *Phys. Rev. E* **59**, 2942 (1999).
- [27] A. S. Bakai, *Low Temp. Phys.* **22**, 733 (1996).
- [28] A. S. Bakai, *Low Temp. Phys.* **24**, 20 (1998).
- [29] E. W. Fischer and A. S. Bakai, in *Slow Dynamics in Complex Systems*, edited by M. Tokuyama and I. Oppenheim, AIP Conf. Proc. No. 469 (AIP Press, New York, 1999), pp. 325–338.
- [30] E. Eckstein, J. Qian, R. Hentschke, T. Thurn-Albrecht, W. Steffen, and E. W. Fischer, *J. Chem. Phys.* **113**, 4751 (2000).